ChemComm

Cite this: *Chem. Commun.*, 2011, **47**, 2396–2398

www.rsc.org/chemcomm

COMMUNICATION

Controlled way to prepare quasi-1D nanostructures with complex chemical composition in porous anodic alumina†

Maria R. Lukatskaya,*[a] Lev A. Trusov,[a] Andrey A. Eliseev,[a] Alexey V. Lukashin,[a] Martin Jansen,[b] Pavel E. Kazin[c] and Kirill S. Napolskii[ac]

Received 13th October 2010, Accepted 27th November 2010
DOI: 10.1039/c0cc04394j

Herein we propose a novel approach to the preparation of quasi-1D nanostructures with various chemical compositions based on infiltration of colloidal solution into the asymmetric anodic alumina membrane. The proposed technique was successfully applied for the preparation of ordered arrays of the magnetically hard anisotropic hexaferrite nanostructures.

One-dimensional nanostructures have attracted close attention of researchers owing to a number of unusual properties that arise from the convolution of dimensionality and particle size effects. It makes these systems essential for both fundamental science and practical applications.[1–5] One of the most promising methods for their formation is templating by porous frameworks with one-dimensional pores. Using anodic aluminium oxide (AAO) as a template, arrays of nanowires[6–8] and nanotubes[9–12] were obtained. This matrix has an ordered array of cylindrical channels with a diameter and an interpore distance easily tuned by varying anodization conditions,[13–15] which makes AAO membranes a universal template material for numerous functional nanostructures.

The electrochemical synthesis inside AAO templates is one of the most efficient methods of controlled growth of nanowires since it provides almost complete filling of the porous framework. In spite of all advantages of electrodeposition, there are some fundamental limitations of this method. It works well for growing metal nanowires,[16–19] while the fabrication of complex phases becomes more problematic and usually requires special procedures to be applied.[20] Therefore, despite existence of the various synthetic techniques that allows us to obtain huge variety of the functional materials there is still a gap that corresponds to the controlled synthesis of the nanorods and nanowires with the complex chemical composition.

Strontium M-type hexaferrite is a magnetically hard material, which has been widely used for permanent magnet production. It exhibits a large magnetocrystalline anisotropy, high Curie temperature, as well as chemical stability and corrosion resistance.[21] Partial substitution of Fe with Al increases its anisotropy field,[22,23] making such hexaferrite phases attractive for practical applications in modern technology (*e.g.* magnetic information storage, MEMS, microwave devices).

Porous anodic alumina films were previously shown to induce magnetic shape anisotropy in metal nanowires and tubes grown in AAO channels.[5] However, no significant magnetic anisotropy was reported for ferrite phases grown in anodic alumina including $CoFe_2O_4$ nanowire[24,25] and nanotube arrays,[26] Fe_3O_4 one dimensional nanostructures[27,28] and Co_3O_4 nanorods.[29]

In this communication, we report on a simple method that allows filling of the AAO membrane with a wide range of substances using enforced infiltration of colloidal nanoparticles. As a testing system we have chosen strontium hexaferrite nanoplatelets that possess pronounced shape and magnetocrystalline anisotropy which allows us to examine the effect of spatial restrictions on the organization of the particles.

Nanocomposite synthesis was performed by filtration of $SrFe_{12-x}Al_xO_{19}$ colloidal solutions through the asymmetric anodic alumina membrane under argon pressure of 7 atm. As the single-crystalline $SrFe_{12-x}Al_xO_{19}$ nanoparticles possessed platelet shape (TEM images are presented in Fig. S1, ESI†), in the case of immobilization of the particles in cylindrical channels of anodic alumina, different mutual orientations of the nanoplatelets can be anticipated. Particles with a different diameter ($D_{particles}$) were introduced into anodic alumina membranes with the same average pore diameter (D_{pores}) in order to investigate particles' mutual orientation in channels depending on the $D_{pores}/D_{particles}$ ratio and its influence on the functional properties of the resulting nanocomposites. Two colloidal solutions of $SrFe_{12-x}Al_xO_{19}$ nanoparticles prepared under almost the same synthetic conditions (more experimental details are presented in Section S1, ESI†) were labeled as 'solution 1' and 'solution 2'. According to TEM and dynamic light scattering data nanoplatelets in 'solution 1' had an average thickness of 5 nm and an average diameter of 60 nm, particles from solution 2 had an average thickness of 7 nm and an average diameter of 80 nm. The coercive force was 4500 and 5600 Oe for particles obtained from the solutions 1 and 2, respectively.

[a] *Department of Materials Science, Moscow State University, 119991 Moscow, Russia. E-mail: lukatskaya@inorg.chem.msu.ru; Fax: +7 4959390998; Tel: +7 4959395248*
[b] *Max-Planck-Institut für Festkörperforschung, D-70569, Stuttgart, Germany*
[c] *Department of Chemistry, Moscow State University, 119991, Moscow, Russia*

† Electronic supplementary information (ESI) available: Experimental details including the synthesis and characterization of the hexaferrite nanoparticles and anodic alumina films. See DOI: 10.1039/c0cc04394j

As the size of the hexaferrite particles was up to 100 nm, the membranes with relatively large pores were required. For this purpose the hard anodization technique in aqueous–alcoholic solutions was applied.[14] Formation of the main part of the membrane was performed using a 150 V anodization regime (for more details see Section S2, ESI†) giving as a result a porous alumina layer with the honey-comb structure and an average interpore distance of 330 nm and a pore diameter of 210 nm (SEM image and interpore distance distribution are shown in Fig. S2, ESI†), which are typical for the applied anodization conditions.[30] In order to prevent a through passage of the colloidal particles under an external pressure, a layer (so called 'blocking layer') with a diameter smaller than the diameter of the nanoparticles was grown from the bottom side of the membrane. In order to obtain the 'blocking layer' the voltage was decreased from 150 V to 75 V for 1 h. The magnetic nanocomposites obtained using solution 1 and solution 2 were labeled as HFS1_AAO and HFS2_AAO, respectively. The principal illustration of the nanocomposites preparation procedure is represented in Scheme 1.

According to SEM, immobilization of the particles took place before the 'blocking layer' leading to the formation of extended stacked aggregates (Fig. 1). Here the blocking layer plays a key role—being an obstacle for the particles to penetrate through the membrane, it allows the solvent to leave freely from the composite.

For a better visualization of the structures formed from the $SrFe_{12-x}Al_xO_{19}$ nanoplatelets inside the anodic alumina membrane the matrix was dissolved in 1 M NaOH aqueous solution and the precipitate was washed with water and dried in air at 60 °C. It should be noted that before the extraction of $SrFe_{12-x}Al_xO_{19}$ nanostructures from the oxide matrix, the composites were annealed in air at 700 °C for 2 h in order to enhance contact between hexaferrite nanoparticles. As an alternative way to protect nanorods from the fragmentation creation of the carbon layer on the walls of anodic alumina channels[31]and thus encapsulation of the colloidal particles inside carbon nanotubes[32] can be suggested. The SEM and TEM images of the extracted hexaferrite nanorods are shown in Fig. 2a and b.

The aggregates turned out to be long rods of densely packed nanoplatelets with an average length exceeding 20 μm. The diameter of the rods was consistent with the pore diameter in

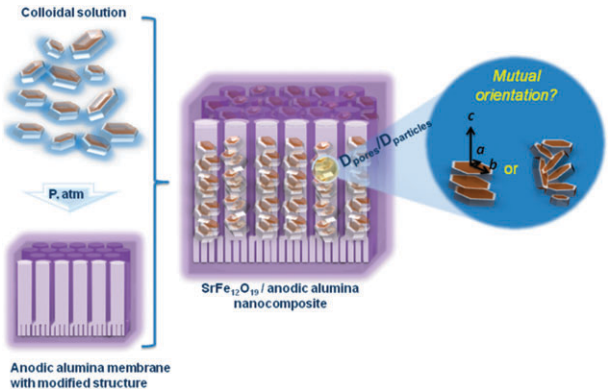

Scheme 1 The schematic view of the colloidal particle immobilization in the asymmetric anodic alumina membrane.

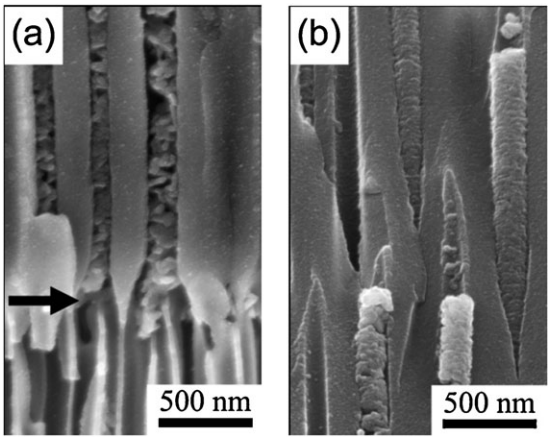

Fig. 1 Cross-sectional view of the HFS1_AAO nanocomposite near the blocking layer (a) and in the middle of the porous alumina membrane (b). The arrow indicates the border of the blocking layer.

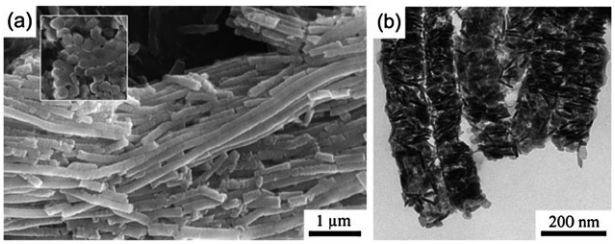

Fig. 2 (a) SEM image of $SrFe_{12-x}Al_xO_{19}$ rods derived from the HFS1_AAO sample with the blocking layer. The inset represents a bundle of rods (top view). (b) TEM image of $SrFe_{12-x}Al_xO_{19}$ rods derived from the HFS1_AAO sample with the blocking layer.

the AAO matrix (see the inset in Fig. 2a). TEM data illustrate that the platelets were oriented preferably with their normal vector along the longitudinal axis of a nanorod. At the lateral surface some nanoparticles lay with their plane along the rod.

Since strontium hexaferrite has one easy magnetization axis parallel to the *c*-axis of the unit cell,[21] preferable orientation of platelets in a composite should produce the magnetic anisotropy in the $SrFe_{12-x}Al_xO_{19}$/AAO nanocomposite.

Indeed, noticeable anisotropy was observed in the field dependence of magnetization (Fig. 3a). The remanent magnetization and coercivity increased when the field was directed at right angle to the membrane surface (along the pores). This implies that the particles on average were preferably oriented with their basal

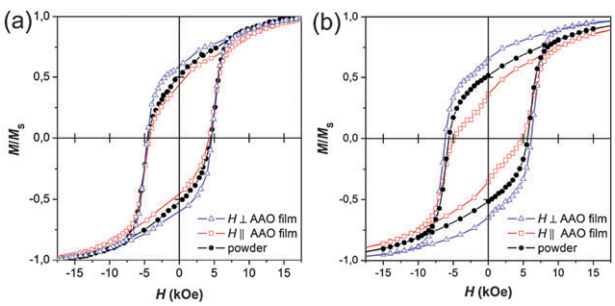

Fig. 3 Magnetic hysteresis loops of HFS1_AAO (a) and HFS2_AAO (b) nanocomposites at different field directions in comparison with the unordered powder.

Table 1 Magnetic properties of $SrFe_{12-x}Al_xO19$/AAO nanocomposites and corresponding hexaferrite powders

	HFS1_AAO		HFS2_AAO	
	H_c/Oe	M_r/M_s	H_c/Oe	M_r/M_s
H is normal to the membrane surface	4600	0.59	6150	0.65
H is parallel to the membrane surface	4250	0.43	4800	0.36
Powder	4500	0.51	5600	0.51

planes (*ab*-planes) perpendicular to the nanorod axis. However the effect is not strong enough in the HFS1_AAO sample and magnetic behavior is close to powder-like.

The reason for the mutual orientation of the particles observed in the rods (Fig. 2b) may be the magnetic dipole–dipole interaction, as every particle is, in fact, a permanent magnet with the direction of spontaneous magnetization normal to the basal plain. Possibly the adhesion forces between the particles and the rheology of the colloid solution also contribute to the process.

The more pronounced magnetic anisotropy was observed for nanocomposite HFS2_AAO based on larger hexaferrite nanoparticles (solution 2) with a higher particle to pore diameter ratio (Fig. 3b). The magnetic characteristics of the obtained samples have been summarized in Table 1.

A larger particle size resulted in a better stacking of the platelets (Fig. 4), giving higher magnetic anisotropy.

Thus, the variation of the particle size to pore diameter ratio enabled the control of the morphology and functional properties of the resulting composites.

In summary, utilization of the blocking layer allows the process of the pores filling to be controlled and to produce ordered arrays of quasi-1D nanostructures. Furthermore, the anisotropic platelet shape of the particles forces them to organize parallel to each other and perpendicular to the direction of a pore. Magnetization measurements demonstrate anisotropic magnetic behavior of the nanocomposites owing to the mutual orientation of the particles.

The synthetic procedure is universal and can be applied to the preparation of a wide range of complex composite materials based on anodic alumina films and other porous media with one-dimensional channels. The proposed technique was first successfully applied for the formation of the ordered arrays of hard magnetic strontium hexaferrite nanorods.

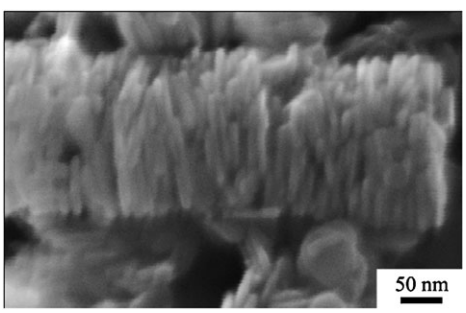

Fig. 4 SEM image of the nanorod fragment extracted from the HFS2_AAO nanocomposite.

This work is partially supported by RF President Grant MK-6626.2010.3, by RFBR (Grant Nos. 08-03-91950 and 09-03-01123) and by DFG project No. 436 RUS 113/933/0-1.

Notes and references

1 H. A. Nilsson, C. Thelander, L. E. Fröberg, J. B. Wagner and L. Samuelson, *Appl. Phys. Lett.*, 2006, **89**, 163101.
2 N. Fu, Z. Li, A. Myalitsin, M. Scolari, R. T. Weitz, M. Burghard and A. Mews, *Small*, 2010, **6**, 376.
3 Y. Xia, P. Yang, Y. Sun, Y. Wu, B. Mayers, B. Gates, Y. Yin, F. Kim and H. Yan, *Adv. Mater.*, 2003, **15**, 353.
4 L. Samuelson, C. Thelander, M. T. Bjork, M. Borgstrom, K. Deppert, K. A. Dick, A. E. Hansen, T. Martensson, N. Panev, A. I. Persson, W. Seifert, N. Skold, M. W. Larsson and L. R. Wallenberg, *Physica E (Amsterdam)*, 2004, **25**, 313.
5 L. Sun, Y. Hao, C.-L. Chien and P. C. Searson, *IBM J. Res. Dev.*, 2005, **49**, 79.
6 G. S. Wu, Y. L. Zhuang, Z. Q. Lin, X. Y. Yuan, T. Xie and L. D. Zhang, *Physica E (Amsterdam)*, 2006, **31**, 5.
7 Y. Zhang, G. H. Li, Y. C. Wu, B. Zhang, W. H. Song and L. Zhang, *Adv. Mater.*, 2002, **14**, 1227.
8 P. Evans, W. R. Hendren, R. Atkinson, G. A. Wurtz, W. Dickson, A. V. Zayats and R. J. Pollard, *Nanotechnology*, 2006, **17**, 5746.
9 M. Steinhart, R. B. Wehrspohn, U. Gosele and J. H. Wendorff, *Angew. Chem., Int. Ed.*, 2004, **43**, 1334.
10 W. Lee, R. Scholz, K. Nielsch and U. Gosele, *Angew. Chem., Int. Ed.*, 2005, **44**, 6050.
11 H. Tsuchiya, J. M. Macak, I. Sieber and P. Schmuki, *Small*, 2005, **1**, 722.
12 A. Johansson, E. Widenkvist, J. Lu, M. Boman and U. Jansson, *Nano Lett.*, 2005, **5**, 1603.
13 J. P. O'Sullivan and G. C. Wood, *Proc. R. Soc. London, Ser. A*, 1970, **317**, 511.
14 W. Lee, R. Ji, U. G. Sele and K. Nielsch, *Nat. Mater.*, 2006, **5**, 741.
15 K. Nielsch, J. Choi, K. Schwirn, R. B. Wehrspohn and U. Gösele, *Nano Lett.*, 2002, **2**, 677.
16 X. Y. Zhang, G. H. Wen, Y. F. Chan, R. K. Zheng, X. X. Zhang and N. Wang, *Appl. Phys. Lett.*, 2003, **83**, 3341.
17 K. S. Napolskii, P. J. Barczuk, S. Yu. Vassiliev, A. G. Veresov, G. A. Tsirlina and P. J. Kulesza, *Electrochim. Acta*, 2007, **52**, 7910.
18 T. M. Whitney, J. S. Jiang, P. C. Searson and C. L. Chien, *Science*, 1993, **126**, 1316.
19 K. S. Napolskii, A. A. Eliseev, N. V. Yesin, A. V. Lukashin, Yu. D. Tretyakov, N. A. Grigorieva, S. V. Grigoriev and H. Eckerlebe, *Physica E (Amsterdam)*, 2007, **37**, 178.
20 Y. Piao, H. Lim, J. Y. Chang, W.-Y. Lee and H. Kima, *Electrochim. Acta*, 2005, **50**, 2997.
21 T. Koutzarova, S. Kolev, C. Chelev, K. Grigorov and I. Nedkov, in *Advances in Nanoscale Magnetism*, ed. B. Aktas and F. Mikailov, Springer, Berlin, Heidelberg, Germany, 2008, Ch. 10.
22 H. Kojima, in *Ferromagnetic Materials*, ed. E. P. Wohlfarth, North-Holland Publishing Company, Amsterdam, 1982, vol. 3.
23 P. E. Kazin, L. A. Trusov, D. D. Zaitsev, Yu. D. Tretyakov and M. Jansen, *J. Magn. Magn. Mater.*, 2008, **320**, 1068.
24 G. Ji, S. Tang, B. Xu, B. Gu and Y. Du, *Chem. Phys. Lett.*, 2003, **379**, 484.
25 Z. H. Hua, R. S. Chen, C. L. Li, S. G. Yang, M. Lu, B. X. Gu and Y. W. Du, *J. Alloys Compd.*, 2007, **427**, 199.
26 Y. Xu, J. Wei, J. Yao, J. Fu and D. Xue, *Mater. Lett.*, 2008, **62**, 1403.
27 T. Wang, Y. Wang, F. Li, C. Xu and D. Zhou, *J. Phys.: Condens. Matter*, 2006, **18**, 10545.
28 S. U. Lian, Z. H. Kang, E. B. Wang, M. Jiang, C. W. Hu and L. Xu, *Solid State Commun.*, 2003, **127**, 605.
29 Y. K. Liu, G. H. Wang, C. K. Xu and W. Z. Wang, *Chem. Commun.*, 2002, 1486.
30 Y. B. Li, M. J. Zheng and L. Ma, *Appl. Phys. Lett.*, 2007, **91**, 073109.
31 T. Kyotani, L. F. Tsai and A. Tomita, *Chem. Mater.*, 1996, **8**, 2109–2113.
32 G. Korneva, H. Ye, Y. Gogotsi, D. Halverson, G. Friedman, J.-C. Bradley and K. G. Kornev, *Nano Lett.*, 2005, **5**, 878.

